Ratio effect of salt fluxes on structure, dielectric and magnetic properties of La,Mn-doped PbBi2Nb2O9 Aurivillius phase

Wendari, Tio Putra; Arief, Syukri; Mufti, Nandang; Baas, Jacob; Blake, Graeme R.; Zulhadjri, [No Value]

Published in:
Ceramics International

DOI:
10.1016/j.ceramint.2020.03.007

Publication date:
2020

Ceramics International 46 (2020) 14822–14827

Contents lists available at ScienceDirect

Ceramics International

journal homepage: www.elsevier.com/locate/ceramint

Ratio effect of salt fluxes on structure, dielectric and magnetic properties of La,Mn-doped $PbBi_2Nb_2O_9$ Aurivillius phase

Tio Putra Wendari[a], Syukri Arief[a], Nandang Mufti[b], Jacob Baas[c], Graeme R. Blake[c], Zulhadjri[a,*]

[a] Department of Chemistry, Faculty of Mathematics and Natural Sciences, Universitas Andalas, Kampus Limau Manis, Padang, 25163, Indonesia
[b] Department of Physics, Faculty of Mathematics and Natural Sciences, Universitas Negeri Malang, Jl. Semarang 5, Malang, 65145, Indonesia
[c] Zernike Institute for Advanced Materials, University of Groningen, Nijenborgh 4, 9747, AG Groningen, the Netherlands

ARTICLE INFO

Keywords:
Aurivillius phase
Molten salt method
Ferroelectric behavior
Double-exchange interaction

ABSTRACT

The double-layer Aurivillius phase $Pb_{0.4}Bi_{2.1}La_{0.5}Nb_{1.7}Mn_{0.3}O_9$ was synthesized by a molten salt method using a K_2SO_4/Na_2SO_4 flux. The effect on the crystal structure, morphology, dielectric and magnetic properties of varying the molar ratio of the oxide precursors to salt flux was investigated. Single-phase products with an orthorhombic structure were obtained for oxide to salt ratios of between 1:5 and 1:9, whereas for lower concentrations of salt a pyrochlore impurity phase is found in the products. SEM showed anisotropic plate-like grains, the size of which increases for larger salt ratios. An investigation of the magnetic properties showed the presence of mixed Mn^{3+} and Mn^{4+}; the unit cell volume of the single-phase products decreases as the proportion of salt increases, which implies a higher proportion of smaller Mn^{4+} cations. This can be explained by the oxide ion donating properties (oxobasicity) of the molten salt mixture, which produces an oxidizing environment during synthesis. The best dielectric properties are obtained for an oxide to salt ratio of 1:7, exhibiting relaxor ferroelectric behavior. This is also the ratio at which the most pronounced ferromagnetic properties are observed, resulting from double-exchange interactions between Mn^{3+} and Mn^{4+}, the proportions of which are approximately equal. $Pb_{0.4}Bi_{2.1}La_{0.5}Nb_{1.7}Mn_{0.3}O_9$ synthesized under these conditions thus exhibits optimal multiferroic properties.

1. Introduction

Ferroelectric materials belonging to the Aurivillius family have attracted much attention due to their high dielectric constants, large remanent polarization, low coercive fields, and high Curie temperatures, material properties that have potential use in random access memory (RAM) [1,2]. The Aurivillius structure is constructed by alternating perovskite blocks and bismuth oxide layers and can be represented by the general formula $(Bi_2O_2)^{2+}(A_{m-1}B_mO_{3m+1})^{2-}$, where A is a mono-, di-, or trivalent cation with dodecahedral coordination, B is a transition metal cation with octahedral coordination, and m is the number of octahedral layers within the perovskite-like blocks [3,4].

The ferroelectric Aurivillius compound $PbBi_2Nb_2O_9$ ($m = 2$) adopts a non-centrosymmetric crystal structure with the $A2_1am$ space group, and exhibits a high Curie temperature (T_c = 557 °C) due to the $6s^2$ lone pair electrons associated with Pb^{2+} and Bi^{3+}, which induce a highly distorted structure [5,6]. Studies with the aim of improving the properties of Aurivillius compounds have been conducted for decades, and the focus in recent years has been especially on possible multiferroic properties. The substitution of a d^n (n ≠ 0) cation on the perovskite B-site can potentially induce a ferromagnetic ordering [2,7]. Besides, the substitution of d^n cations might also result in a distortion of the BO_6 octahedra due to the effect of different ionic radii on the B-site, thus enhancing the ferroelectric properties [8,9]. Furthermore, the substitution of lanthanide ions on the perovskite A-site is well known in Aurivillius phases to improve the dielectric and piezoelectric properties, reduce the electrical conductivity and dielectric loss, and possibly lead to relaxor-ferroelectric behavior [10,11]. Therefore, the simultaneous substitution of both La^{3+} and Mn^{3+} (d^4) ions can potentially result in multiferroic properties, which is beneficial for the application of non-volatile memory.

Aurivillius phases are usually prepared by solid-state synthesis. However, the synthesis of single-phase multiferroic Aurivillius samples is challenging because impurities tend to be formed due to the different character of the transition metal d-orbitals and the difference in ionic radii when partial substitutions are performed [12]. High-temperature

* Corresponding author. Department of Chemistry, Faculty of Mathematics and Natural Sciences, Universitas Andalas, Kampus Limau Manis, Padang, 25163, Indonesia.
E-mail address: zulhadjri@sci.unand.ac.id (Zulhadjri).

https://doi.org/10.1016/j.ceramint.2020.03.007
Received 10 January 2020; Received in revised form 29 February 2020; Accepted 1 March 2020
Available online 02 March 2020

synthesis often leads to the volatilization of Bi^{3+} which requires the addition of excess Bi_2O_3 to the precursor mixture [13]. In many cases synthesis using a molten salt method is superior; the use of salt fluxes as the reaction medium gives many advantages such as lower-temperature synthesis, fast ionic diffusion, and high reaction rates [14]. Molten sulfate and chloride salts have been widely applied to synthesize multiferroic Aurivillius phases [8,15,16]. The precise nature of the salt flux plays a crucial role in determining the compositional and grain homogeneity of the product, which in turn strongly affects the physical properties. However, many reports on the molten salt synthesis of Aurivillius phases only focus on the role of the salt flux in the growth mechanism. Thus, our research aim is to determine the best flux ratio for obtaining single-phase products and optimal multiferroic properties.

Recently, we have reported on the preparation of the La,Mn-doped $PbBi_2Nb_2O_9$ phase with chemical formula $Pb_{1-2x}Bi_{1.5+2x}La_{0.5}Nb_{2-x}Mn_xO_9$ using a K_2SO_4/Na_2SO_4 molten salt flux with a ratio of 1:7 oxide to salt [17]. A single-phase product was obtained for the maximum achievable Mn content of $Pb_{0.4}Bi_{2.1}La_{0.5}Nb_{1.7}Mn_{0.3}O_9$, which exhibits the best dielectric properties of this doping series and exhibit the pronounced ferromagnetic properties [18]. This compound is also interesting to explore because of the reduced lead content which represents a more environmentally friendly material compared to $PbBi_2Nb_2O_9$. Therefore, we continue our studies of this material by investigating the effect of the oxide to salt ratio on the purity, crystal structure, morphology, dielectric and magnetic properties. The molar ratio of oxide to salt was varied from 1:0 to 1:9.

2. Experimental procedures

The precursors PbO, Bi_2O_3, La_2O_3, Nb_2O_5, and Mn_2O_3 (Aldrich, ≥ 99.9%) were weighed in a stoichiometric ratio for the target formula $Pb_{0.4}Bi_{2.1}La_{0.5}Nb_{1.7}Mn_{0.3}O_9$ and mixed and ground in an agate mortar with added ethanol for 2 h. A 1:1 molar ratio of K_2SO_4/Na_2SO_4 salts was then added to the precursor mixture to give molar ratios of oxide to salt of 1:0, 1:3, 1:5, 1:7, and 1:9, denoted as samples PBLNM0, PBLNM3, PBLNM5, PBLNM7, and PBLNM9, respectively. The mixtures were successively calcined at 750 °C, 850 °C and 950 °C for 5 h each with a heating rate of 5 °C/min. After heating at each temperature, the powders were slowly cooled to room temperature and reground. The products were finally washed several times with hot distilled water to remove the sulfate salts and then dried at 110 °C for 5 h. The crystalline phases in the products were analyzed by X-ray diffraction (Shimadzu XRD 7000). The unit cells were refined by the Le Bail refinement technique using the RIETICA program. Scanning electron microscopy (FEI INSPECT S50) was used to observe the grain morphology. For dielectric measurements, the powder was pressed into pellets and sintered at 900 °C for 5 h. Silver conductive paste (Aldrich, 99%) was applied to both surfaces of the sintered pellet to form electrodes and heated at 110 °C for 2 h. The dielectric measurements were carried out using a precision LCR-meter (Agilent 4980A) with an amplitude of 1 V in the temperature range 30 to 500 °C at a frequency of 1 MHz. The magnetization was measured using a SQUID magnetometer (Quantum Design MPMS XL7) in the temperature range from 5 to 300 K under a magnetic field of 1 T. Magnetization as a function of applied field was measured from -5 T to 5 T at a temperature of 5 K.

3. Results and discussion

Fig. 1 shows XRD patterns of $Pb_{0.4}Bi_{2.1}La_{0.5}Nb_{1.7}Mn_{0.3}O_9$ synthesized using varying salt ratios. All the XRD patterns are indexed using the standard pattern of the double-layer Aurivillius phase $PbBi_2Nb_2O_9$, which has an orthorhombic structure with the $A2_1am$ space group (ICSD-95920). Single-phase products were obtained for PBLNM5, PBLNM7 and PBLNM9, while for PBLNM0 and PBLNM3 a pyrochlore impurity phase was detected. The formation of the pyrochlore phase might be caused by bismuth volatilization during high-temperature processing [15,19]. It is expected that the salt flux plays a crucial role as a reaction medium, enhancing the solubility of the oxide precursors, facilitating ion diffusion and suppressing Bi^{3+} volatilization. Moreover, the formation of single-phase $Pb_{0.4}Bi_{2.1}La_{0.5}Nb_{1.7}Mn_{0.3}O_9$ suggests that 0.5 moles of La^{3+} can be incorporated on the *A*-site of $PbBi_2Nb_2O_9$ and 0.3 moles of Mn^{3+} on the *B*-site, and that a minimum ratio of oxide to salt of 1:5 is required.

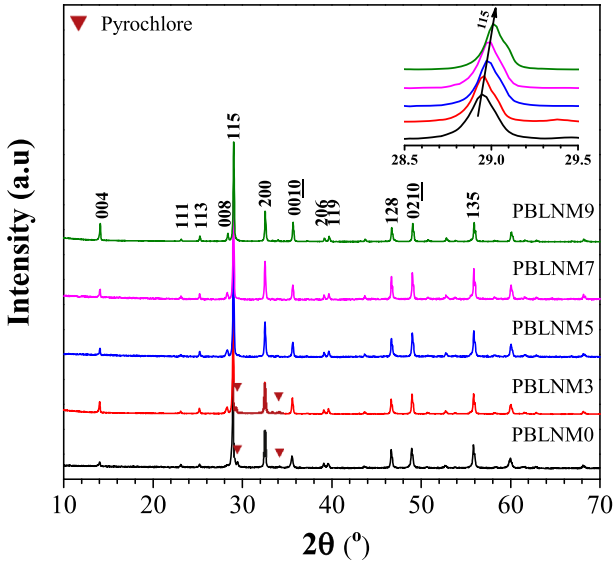

Fig. 1. XRD patterns of $Pb_{0.4}Bi_{2.1}La_{0.5}Nb_{1.7}Mn_{0.3}O_9$ powders prepared by the molten salt method with different oxide to salt ratios.

With increasing salt ratio, the full width at half maximum (FWHM) of the XRD peaks decreases, indicating an increase in crystallinity. The average crystallite size calculated using Scherrer's formula is approximately 48 nm, 56 nm, 65 nm, 67 nm and 69 nm for samples PBLNM0, PBLNM3, PBLNM5, PBLNM7, and PBLNM9, respectively. These results suggest that the salt flux accelerates grain growth during the heating process [20]. It is also observed (see the inset of Fig. 1) that the most intense diffraction peak (115) shifts to higher 2θ with increasing salt ratio, implying a decrease in lattice parameters and cell volume.

The effect of the salt ratio on the grain size and morphology of $Pb_{0.4}Bi_{2.1}La_{0.5}Nb_{1.7}Mn_{0.3}O_9$ was investigated using SEM as shown in Fig. 2. Anisotropic plate-like grains are observed for all samples, which is typical for Aurivillius phases. However, both the size and morphology are significantly affected by the salt ratio. The average grain size of PBLNM0 is approximately 1.0 μm with the highest degree of agglomeration. As the salt ratio increases, the average grain size increases to 1.6 μm, 1.8 μm, 2.3 μm, and 2.4 μm for PBLNM3, PBLNM5, PBLNM7, and PBLNM9, respectively. Moreover, a decrease in agglomeration is observed and the grain shape becomes more uniform. It is known that grain growth is accelerated when salt fluxes are used as the reaction medium, leading to larger grain sizes when the proportion of salt used is higher [21]. Furthermore, the flux diffuses between the grains and prevents the occurrence of agglomeration at higher salt ratios [20].

Refinement of the lattice parameters was carried out using the Le Bail method only for the single-phase products PBLNM5, PBLNM7 and PBLNM9, using the structural parameters of orthorhombic $PbBi_2Nb_2O_9$ with space group $A2_1am$ [22] as the initial model. The profile plots in Fig. 3 show good fits for all three samples and suggest that the products also adopt the non-centrosymmetric $A2_1am$ structure of the parent compound. The refined lattice parameters and unit cell volumes are given in Table 1. The *a* and *b* lattice parameters are essentially the same for the three samples, whereas the *c* lattice parameter significantly decreases as the salt ratio increases, leading to a decrease in cell volume. This implies a shrinkage of the BO_6 octahedra due to a shortening of the *B*–O bond lengths and could occur due to a varying proportion of

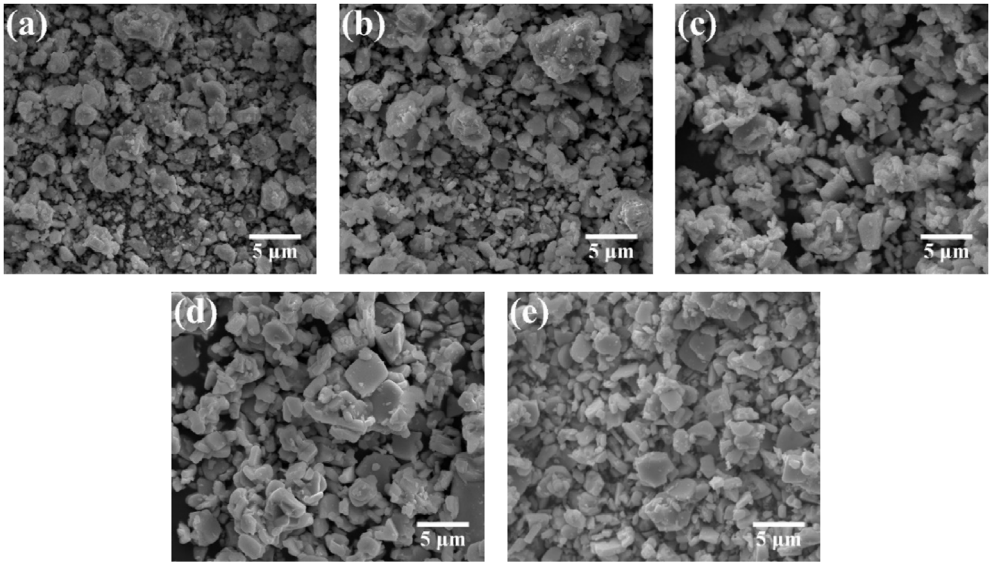

Fig. 2. SEM images of $Pb_{0.4}Bi_{2.1}La_{0.5}Nb_{1.7}Mn_{0.3}O_9$ samples: **(a)** PBLNM0, **(b)** PBLNM3, **(c)** PBLNM5, **(d)** PBLNM7, **(e)** PBLNM9.

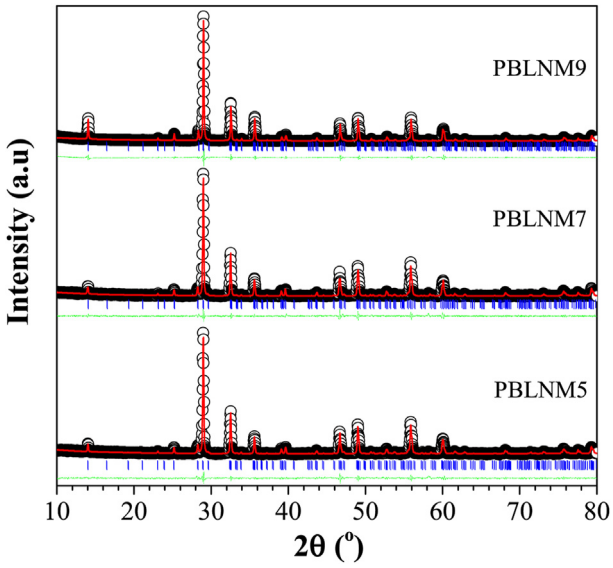

Fig. 3. Le Bail fits to XRD data for single-phase $Pb_{0.4}Bi_{2.1}La_{0.5}Nb_{1.7}Mn_{0.3}O_9$ samples: measured data (circles), fitted profile (red line), and difference profile (green line). The blue tick-marks indicate the positions of allowed Bragg reflections in the space group $A2_1am$. (For interpretation of the references to colour in this figure legend, the reader is referred to the Web version of this article.)

Table 1
Structural parameters of single-phase $Pb_{0.4}Bi_{2.1}La_{0.5}Nb_{1.7}Mn_{0.3}O_9$ obtained from XRD fits.

Parameter	PBLNM5	PBLNM7	PBLNM9
Space Group	$A2_1am$	$A2_1am$	$A2_1am$
Crystal class	Orthorhombic	Orthorhombic	Orthorhombic
a (Å)	5.5173(7)	5.5190(4)	5.5166(0)
b (Å)	5.4911(9)	5.4904(3)	5.4899(3)
c (Å)	25.1909(8)	25.1576(8)	25.1265(3)
V (Å^3)	763.210(3)	762.327(2)	760.977(3)
Z	4	4	4
R_p (%)	2.979	3.219	3.687
R_{wp} (%)	3.901	4.225	4.46
χ^2	1.439	1.560	1.591

Mn^{4+} ions; the ionic radius in six-fold coordination of Mn^{4+} (0.54 Å) is smaller than that of Mn^{3+} (0.645 Å) [23]. The mixed-valent Mn^{3+}/Mn^{4+} state could also be expected to give rise to ferromagnetic ordering via Mn^{3+}-O-Mn^{4+} double-exchange interactions [24], as discussed further below.

Fig. 4a shows the frequency dependence of the dielectric constant (ϵ) and dielectric loss (tan δ) of the single-phase products at room temperature. The dielectric constant decreases up to 100 kHz and then remains stable with further increasing frequency, which is typical behavior in ferroelectric materials. In the low-frequency range, the higher dielectric constant and dielectric loss arise from extrinsic factors, such as the presence of electronic, ionic, dipolar, and space-charge polarization; this is also caused by the Maxwell-Wagner effect, where charge carriers accumulate at the surface and at grain boundaries. The decrease of dielectric constant at high frequencies is because partial polarization mechanisms cannot follow the electric field, such that the main contribution to the dielectric constant is from electronic polarization and ionic polarization.

Fig. 4b shows the temperature dependence of the dielectric constant (ϵ) and dielectric loss (tan δ) of the single-phase products at 1 MHz, which best reflect the intrinsic factors. All samples show a single peak in the dielectric constant at 365 °C, corresponding to the ferroelectric-paraelectric phase transition (T_c). The well-defined peak at T_c indicates the predominance of ferroelectric properties according to $A2_1am$ symmetry in all samples. Compared with the parent compound $PbBi_2Nb_2O_9$ for which T_c = 557 °C [5], the T_c of $Pb_{0.4}Bi_{2.1}La_{0.5}Nb_{1.7}Mn_{0.3}O_9$ is significantly decreased. This is because the substitution of La^{3+} on the A-site, which does not have a lone pair, reduces the degree of BO_6 distortion. Furthermore, the broadness of the T_c peak for all samples indicates relaxor-ferroelectric behavior, unlike the parent compound. This behavior is attributed to the increased disorder of both the A-site cations (Pb/Bi/La) and B-site cations (Nb/Mn) in the structure, as previously reported using neutron diffraction analysis [18].

The magnitude of the dielectric constant initially increases from sample PBLNM5 to PBLMN7 and then decreases for PBLNM9, while the dielectric loss increases linearly with the increase in salt ratio, as shown in Fig. 4a-b. This can be explained by the increasing grain size, which allows the movement of domain walls to become easier and the sample to more readily become polarized, resulting in enhanced dielectric properties [17,25]. We also suggest that the trend in dielectric loss with salt ratio is a consequence of the increasing grain size, as listed in Table 2. Larger grains and hence a decrease in the number of grain boundaries allow the charge carriers to move more freely, contributing

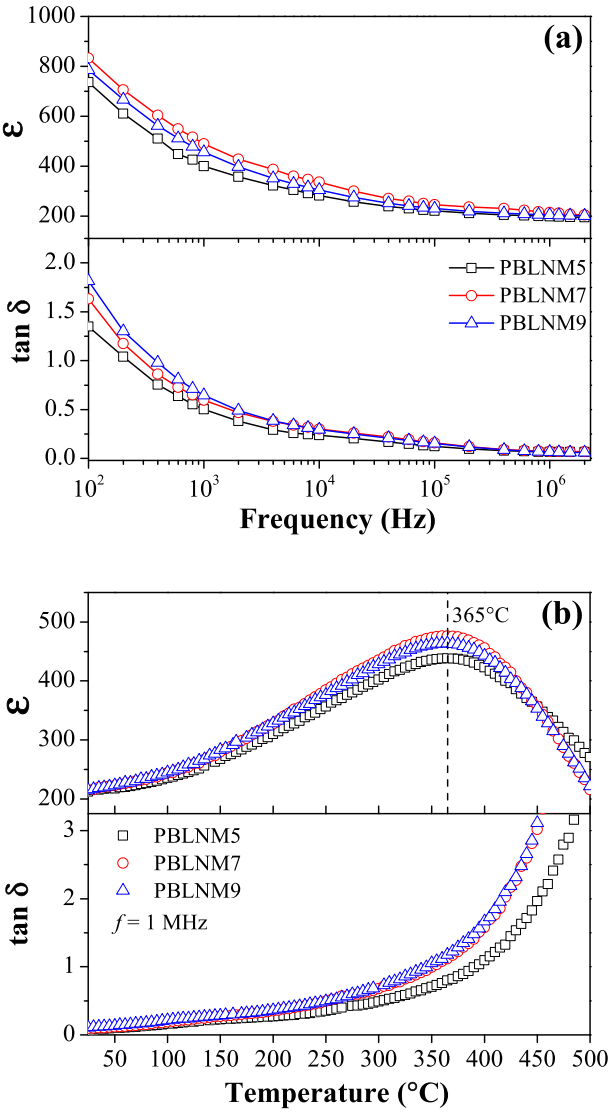

Fig. 4. (a) Dielectric constant (ϵ) and loss (tan δ) of single-phase $Pb_{0.4}Bi_{2.1}La_{0.5}Nb_{1.7}Mn_{0.3}O_9$ as a function of frequency at room temperature **(b)** Dielectric constant (ϵ) and loss (tan δ) of single-phase $Pb_{0.4}Bi_{2.1}La_{0.5}Nb_{1.7}Mn_{0.3}O_9$ as a function of temperature at 1 MHz.

Table 2
Variation of dielectric properties of single-phase samples of $Pb_{0.4}Bi_{2.1}La_{0.5}Nb_{1.7}Mn_{0.3}O_9$ measured at 1 MHz.

Sample	Grain size (μm)	T_c (°C)	ε_m	tan δ
PBLNM5	~1.8	365	438.39	0.801
PBLNM7	~2.3	365	476.14	1.079
PBLNM9	~2.4	365	463.47	1.179

to the increase in dielectric loss. These results may also be influenced by the hopping conduction of electrons associated with double exchange via Mn^{3+}-O-Mn^{4+} bonds. As explained above, samples prepared with a higher salt ratio show an increase in the proportion of Mn^{4+} ions.

In order to investigate the magnetic behavior of the $Pb_{0.4}Bi_{2.1}La_{0.5}Nb_{1.7}Mn_{0.3}O_9$ samples, the temperature dependence of the magnetic susceptibility (χ) was measured in zero-field-cooled (ZFC) mode on warming in an applied magnetic field of 1 T. Fig. 5a shows that the magnetic susceptibility smoothly decreases with increasing temperature and does not exhibit any anomalies, suggesting paramagnetic behavior. A Curie-Weiss fit to the linear region of the inverse

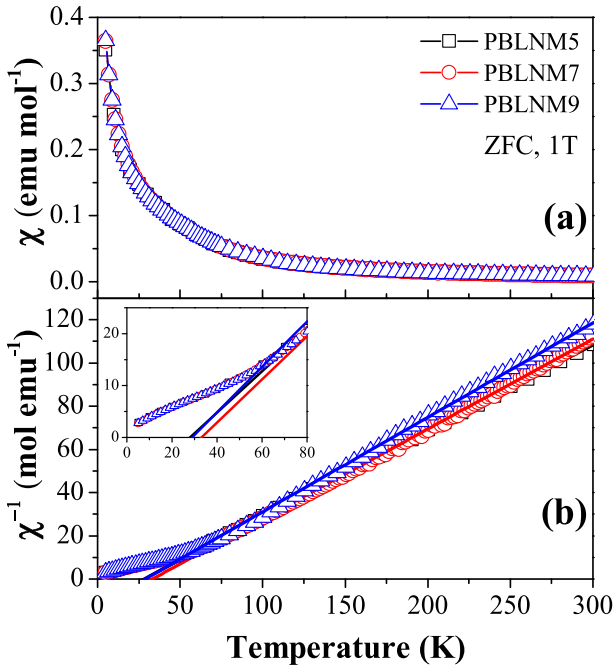

Fig. 5. (a) Magnetic susceptibility (χ) and **(b)** inverse magnetic susceptibility ($1/\chi$) of single-phase $Pb_{0.4}Bi_{2.1}La_{0.5}Nb_{1.7}Mn_{0.3}O_9$ measured from 5 to 300 K in an applied field of 1 T (after cooling in zero field). The straight lines are linear fits to the inverse susceptibility above 150 K using the Curie-Weiss law.

Table 3
Magnetic properties of single-phase samples of $Pb_{0.4}Bi_{2.1}La_{0.5}Nb_{1.7}Mn_{0.3}O_9$.

Sample	θ_{CW} (K)	μ_{eff} (μ_B)	M_s (emu g^{-1})	M_r (emu g^{-1})
PBLNM5	28.0	4.48	3.47	0.0069
PBLNM7	33.4	4.38	3.48	0.0103
PBLNM9	28.9	4.27	3.48	0.0087

susceptibility above 150 K was performed, as shown in Fig. 5b. The extracted Curie-Weiss temperatures (θ_{CW}) are positive for all the single-phase samples, as observed in the inset of Fig. 5b and listed in Table 3, indicating the predominance of ferromagnetic interactions. The largest θ_{CW} value of 33.4 K is found for sample PBLNM7, implying the most pronounced ferromagnetic interactions.

The spin-only effective moments (μ_{eff}) of Mn for the single-phase samples extracted from the Curie-Weiss fitting are listed in Table 3. The values lie between those expected for Mn^{3+} (~4.9 μ_B) and Mn^{4+} (~3.87 μ_B) [26,27]. Thus, all samples contain a mixture of both cations. The decrease in μ_{eff} with increasing oxide to salt ratio confirms that the proportion of Mn^{4+} increases, in agreement with the trend in the *c*-lattice parameter. The PBLNM5 sample contains more Mn^{3+} than Mn^{4+} (60% to 40%), PBLNM7 contains approximately equal proportions of Mn^{3+} and Mn^{4+}, and PBLNM9 contains less Mn^{3+} than Mn^{4+} (39% to 61%).

The tendency of more Mn^{4+} to be stabilized at higher salt ratios might be due to an oxide ion donor mechanism involving oxobasic SO_4^{2-} anions, according to Lux-Flood acid-base theory. It has been reported that molten salt fluxes tend to be oxidizing in solution, leading to products with higher oxidation states [28]. This might be further promoted by the oxygen-rich sintering atmosphere used in the present work. The oxidation of Mn^{3+} in Aurivillius compounds synthesized using the molten salt method has also been observed previously [8]. We note that a varying ratio of Mn^{3+}/Mn^{4+} would require a varying concentration of vacancies on other cation sites to achieve charge balance, an aspect that requires further study.

Mixed-valent Mn^{3+}/Mn^{4+} will enable double-exchange to take

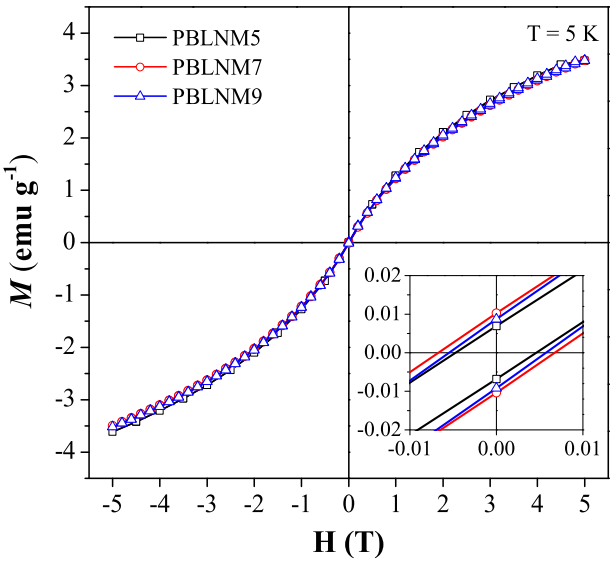

Fig. 6. Magnetization versus applied field for $Pb_{0.4}Bi_{2.1}La_{0.5}Nb_{1.7}Mn_{0.3}O_9$ measured at 5 K.

place, accounting for the ferromagnetic interactions observed in all the samples. However, the presence of double-exchange implies that clusters of linked MnO_6 octahedra exist in the structure, as previously suggested by the Raman mode observed at ~756 cm^{-1} [17]. The equal proportion of Mn^{3+} and Mn^{4+} in the PBLNM7 sample likely results in the highest probability of double-exchange interactions occurring within Mn-rich clusters, as suggested by the highest θ_{CW}. For PBLNM5 and PBLNM9, the higher proportion of either Mn^{3+} or Mn^{4+} will likely favor the antiferromagnetic super-exchange interactions Mn^{3+}-O-Mn^{3+} or Mn^{4+}-O-Mn^{4+}, leading to a decrease of θ_{CW}. It has commonly been observed that ferromagnetic behavior can be enhanced by combining mixed-valent magnetic cations in an equal ratio [29,30]. However, no ferromagnetic-paramagnetic transition peak (T_c) is observed in Fig. 5a because the total Mn-content is far below the percolation threshold for long-range magnetic ordering.

In order to verify the existence of ferromagnetic interactions, the magnetic field dependence of the magnetization was measured at a temperature of 5 K, as shown in Fig. 6. The magnetization increases with magnetic field in non-linear fashion and remains unsaturated in magnetic fields up to 5 T. A narrow hysteresis loop can be observed in the inset of Fig. 6, providing evidence for ferromagnetic properties. The remnant magnetization (M_r) is highest in the PBLNM7 sample (Table 3) and is consistent with an increased probability of double-exchange interactions as discussed above.

4. Conclusions

The double-layer Aurivillius compound $Pb_{0.4}Bi_{2.1}La_{0.5}Nb_{1.7}Mn_{0.3}O_9$ has been synthesized by a molten salt method using varying proportions of K_2SO_4/Na_2SO_4 flux. Single-phase products are obtained for oxide to salt ratios of 1:5 and higher. As the salt ratio increases, the unit cell volume decreases and the grains become larger with less agglomeration. The best dielectric properties are obtained for a salt ratio of 1:7, which at 1 MHz gives a ferroelectric transition temperature of 365 °C, a maximum dielectric constant of 476.14, and a dielectric loss (tan δ) of 1.079. Magnetic susceptibility measurements demonstrate the presence of mixed-valent Mn^{3+}/Mn^{4+}, where the tendency to stabilize Mn^{4+} increases with the salt ratio. The most pronounced ferromagnetic properties are obtained for a salt ratio of 1:7, as evidenced by the highest θ_{CW} and M_r. In conclusion, the Aurivillius compound $Pb_{0.4}Bi_{2.1}La_{0.5}Nb_{1.7}Mn_{0.3}O_9$ exhibits multiferroic properties, which are optimal when synthesized using a molar oxide to salt ratio of 1:7.

Declaration of competing interest

The authors declare that they have no known competing financial interests or personal relationships that could have appeared to influence the work reported in this paper.

Acknowledgments

This work was supported by the Ministry of Research, Technology and Higher Education (RISTEKDIKTI) of the Republic of Indonesia through the PMDSU Scholarship [Grant number 050/SP2H/LT/DRPM/2018]; and by the PKPI-PMDSU Scholarship [Grant number 1406.29/D3/PG/2018]with the University of Groningen, The Netherlands.

References

[1] J.F.Scott, Ferroelectric Memories, first ed., Springer-Verlag Berlin Heidelberg, New York, n.d. doi:10.1007/978-3-662-04307-3.
[2] W. Eerenstein, N.D. Mathur, J.F. Scott, Multiferroic and magnetoelectric materials, Nature 442 (2006) 759–765, https://doi.org/10.1016/j.actamat.2011.12.024.
[3] B. Aurivillius, Mixed bismuth oxides with layer lattices 1. The structure type of $CaNb_2Bi_2O_9$, Ark. För Kemi. 1 (1949) 463–480.
[4] E.C. Subbarao, A family of ferroelectric bismuth compounds, J. Phys. Chem. Solid. 23 (1962) 665–676, https://doi.org/10.1016/0022-3697(62)90526-7.
[5] H. Du, Y. Li, H. Li, X. Shi, C. Liu, Relaxor behavior of bismuth layer-structured ferroelectric ceramic with m = 2, Solid State Commun. 148 (2008) 357–360, https://doi.org/10.1016/j.ssc.2008.05.017.
[6] Ismunandar, B.A. Hunter, B.J. Kennedy, Cation disorder in the ferroelectric Aurivillius phase $PbBi_2Nb_2O_9$: an anamolous dispersion X-ray diffraction study, Solid State Ionics 112 (1998) 281–289, https://doi.org/10.1016/S0167-2738(98)00222-7.
[7] A.J.C. Buurma, G.R. Blake, T.T.M. Palstra, Multiferroic Materials : Physics and Properties, Elsevier Ltd., 2016, https://doi.org/10.1016/B978-0-12-803581-8.09245-6.
[8] Zulhadjri, B. Prijamboedi, A.A. Nugroho, N. Mufti, A. Fajar, T.T.M. Palstra, Ismunandar, Aurivillius phases of $PbBi_4Ti_4O_{15}$ doped with Mn^{3+} synthesized by molten salt technique: structure, dielectric, and magnetic properties, J. Solid State Chem. 184 (2011) 1318–1323, https://doi.org/10.1016/j.jssc.2011.03.044.
[9] P. Fang, P. Liu, Z. Xi, W. Long, X. Li, Structure and electrical properties of new Aurivillius oxides $(K_{0.16}Na_{0.84})_{0.5}Bi_{4.5}Ti_4O_{15}$ with manganese modification, J. Alloys Compd. 595 (2014) 148–152, https://doi.org/10.1016/j.jallcom.2014.01.152.
[10] A. Khokhar, P.K. Goyal, O.P. Thakur, A.K. Shukla, K. Sreenivas, Influence of lanthanum distribution on dielectric and ferroelectric properties of $BaBi_{4-x}La_xTi_4O_{15}$ ceramics, Mater. Chem. Phys. 152 (2015) 13–25, https://doi.org/10.1016/j.matchemphys.2014.11.074.
[11] S. Liu, S. Yan, H. Luo, L. Yao, Z. Hu, S. Huang, L. Deng, Enhanced magnetoelectric coupling in La-modified $Bi_5Co_{0.5}Fe_{0.5}Ti_3O_{15}$ multiferroic ceramics, J. Mater. Sci. 53 (2018) 1014–1023, https://doi.org/10.1007/s10853-017-1604-6.
[12] B. Prijamboedi, Zulhadjri, A.A. Nugroho, Ismunandar, Synthesis and structure analysis of Aurivillius phases $Pb_{1-x}Bi_{4+x}Ti_{4-x}Mn_xO_{15}$, J. Chin. Chem. Soc. 56 (2009) 1108–1111, https://doi.org/10.1002/jccs.200900160.
[13] J. Xiao, H. Zhang, Y. Xue, Z. Lu, X. Chen, P. Su, F. Yang, X. Zeng, The influence of Ni-doping concentration on multiferroic behaviors in $Bi_4NdTi_3FeO_{15}$ ceramics, Ceram. Int. 41 (2015) 1087–1092, https://doi.org/10.1016/j.ceramint.2014.09.033.
[14] M. García-guaderrama, G. Guadalupe, C. Arizaga, A. Durán, Effect of synthesis conditions on the morphology and crystal structure, Ceram. Int. 40 (2014) 7459–7465, https://doi.org/10.1016/j.ceramint.2013.12.094.
[15] X. Chen, Z. Lu, F. Huang, J. Min, J. Li, J. Xiao, F. Yang, X. Zeng, Molten salt synthesis and magnetic anisotropy of multiferroic $Bi_4NdTi_3Fe_{0.7}Ni_{0.3}O_{15}$ ceramics, J. Alloys Compd. 693 (2017) 448–453, https://doi.org/10.1016/j.jallcom.2016.09.214.
[16] D.G. Porob, P.A. Maggard, Synthesis of textured $Bi_5Ti_3FeO_{15}$ and $LaBi_4Ti_3FeO_{15}$ ferroelectric layered Aurivillius phases by molten-salt flux methods, Mater. Res. Bull. 41 (2006) 1513–1519, https://doi.org/10.1016/j.materresbull.2006.01.020.
[17] T.P. Wendari, S. Arief, N. Mufti, V. Suendo, A. Prasetyo, Ismunandar, J. Baas, G.R. Blake, Synthesis Zulhadjri, Structural analysis and dielectric properties of the double-layer Aurivillius compound $Pb_{1-2x}Bi_{1.5+2x}La_{0.5}Nb_{2-x}Mn_xO_9$, Ceram. Int. 45 (2019) 17276–17282, https://doi.org/10.1016/j.ceramint.2019.05.285.
[18] T.P. Wendari, S. Arief, N. Mufti, A. Insani, J. Baas, G.R. Blake, Zulhadjri, Structural and multiferroic properties in double-layer Aurivillius phase $Pb_{0.4}Bi_{2.1}La_{0.5}Nb_{1.7}Mn_{0.3}O_9$ prepared by molten salt method, J. Alloys Compd. 820 (2020) 153145, https://doi.org/10.1016/j.jallcom.2019.153145.
[19] C. Lu, C. Wu, Preparation, sintering, and ferroelectric properties of layer-structured strontium bismuth titanium oxide ceramics, J. Eur. Ceram. Soc. 22 (2002) 707–714, https://doi.org/10.1016/S0955-2219(01)00377-6.
[20] X. Tian, F. Gao, S. Qu, H. Ma, B. Wang, Effects of molten salt content and reaction temperature on molten salt preparation of $CaNaBi_2Nb_3O_{12}$ powder, J. Mater. Sci. Mater. Electron. 26 (2015) 6189–6193, https://doi.org/10.1007/s10854-015-3201-2.

[21] Z. Zhao, X. Li, H. Ji, M. Deng, Formation mechanism of plate-like $Bi_4Ti_3O_{12}$ particles in molten salt fluxes, Integrated Ferroelectrics 154 (2014) 154–158, https://doi.org/10.1080/10584587.2014.904705.
[22] K. Miura, Electronic properties of ferroelectric $SrBi_2Ta_2O_9$, $SrBi_2Nb_2O_9$, and $PbBi_2Nb_2O_9$ with optimized structures, Appl. Phys. Lett. 80 (2002) 2967–2969, https://doi.org/10.1063/1.1474607.
[23] R.D. Shannon, Revised effective ionic radii and systematic studies of interatomie distances in halides and chaleogenides, Acta Crystallogr. 32 (1976) 751–767.
[24] B. Zhang, C. Cao, G. Li, F. Li, W. Ji, S. Zhang, M. Ren, H. Zhang, R.Q. Zhang, Z. Zhong, Z. Yuan, S. Yuan, G.R. Blake, 2p-insulator heterointerfaces: creation of half-metallicity and anionogenic ferromagnetism via double exchange, Phys. Rev. B 97 (2018) 165109, https://doi.org/10.1103/PhysRevB.97.165109.
[25] X. Tian, S. Qu, H. Ma, Z. Pei, B. Wang, Effect of grain size on dielectric and piezoelectric properties of bismuth layer structure $CaBi_2Nb_2O_9$ ceramics, J. Mater. Sci. Mater. Electron. 27 (2016) 13309–13313, https://doi.org/10.1007/s10854-016-5480-7.
[26] C.A. López, M.E. Saleta, J.C. Pedregosa, R.D. Sánchez, J.A. Alonso, M.T. Fernández-díaz, Cationic disorder and Mn^{3+}/Mn^{4+} charge ordering in the B' and B'' sites of $Ca_3Mn_2NbO_9$ perovskite: a comparison with $Ca_3Mn_2WO_9$, J. Solid State Chem. 210 (2014) 1–9, https://doi.org/10.1016/j.jssc.2013.10.039.
[27] K. Nakade, K. Hirota, M. Kato, H. Taguchi, Effect of the Mn^{3+} ion on electrical and magnetic properties of orthorhombic perovskite-type $Ca(Mn_{1-x}Ti_x)O_{3-\delta}$, Mater. Res. Bull. 42 (2007) 1069–1076, https://doi.org/10.1016/j.materresbull.2006.09.013.
[28] J. Boltersdorf, N. King, P.A. Maggard, Flux-mediated crystal growth of metal oxides: synthetic tunability of particle morphologies, sizes, and surface features for photocatalysis research, CrystEngComm 17 (2015) 2225–2241, https://doi.org/10.1039/c4ce01587h.
[29] C.X. Chen, Y.K. Liu, R.K. Zheng, Magnetic and ferroelectric properties of $SmBi_4Fe_{0.5}Co_{0.5}Ti_3O_{15}$ compounds prepared with different synthesis methods, J. Mater. Sci. Mater. Electron. 28 (2017) 7562–7567, https://doi.org/10.1007/s10854-017-6446-0.
[30] Y. Wu, T. Yao, Y. Lu, B. Zou, X. Mao, F. Huang, H. Sun, X. Chen, Magnetic, dielectric, and magnetodielectric properties of Bi-layered perovskite $Bi_{4.25}Gd_{0.75}Fe_{0.5}Co_{0.5}Ti_3O_{15}$, J. Mater. Sci. 52 (2017) 7360–7368, https://doi.org/10.1007/s10853-017-0971-3.